#76

High-Pressure Researches in Geoscience (editor W. Schreyer), pp. 151–176
E. Schweizerbart'sche Verlagsbuchhandlung, Stuttgart, 1982

SECTION III: STRUCTURAL BEHAVIOUR

High-Temperature and High-Pressure Crystal Chemistry*

R. M. HAZEN and L. W. FINGER

Geophysical Laboratory, Carnegie Institution of Washington, Washington, D. C. 20008, U.S.A.

With 13 figures and 2 tables in the text

Abstract: Studies of mineral crystal structures at elevated temperature and pressure are reviewed. Single-crystal X-ray devices now sustain high temperatures to 1100 °C and pressures to 100 kbar. A heated single-crystal, diamond-anvil pressure cell has achieved 450 °C at 30 kbar. A range of T-P conditions corresponding to a significant portion of the crust and upper mantle may thus be reproduced in single-crystal experiments.

Mean linear thermal expansion, α_{poly}, and compression, β_{poly}, of each type of cation-anion coordination polyhedron are independent of structure. Simple empirical relationships result in the prediction of α_{poly} and β_{poly} from ionic bonding parameters:

$$\alpha_{poly} = 4.0\,(4) \times 10^{-6} \frac{n}{S^2 z_c z_a}\ °C^{-1},$$

and

$$\beta_{poly} = 0.133\,(4)\ (\bar{d}^3/S^2 z_c z_a)\ Mbar^{-1},$$

where n is coordination number, $\bar{d}$ is mean cation-anion bond distance, S is an ionicity term, and z_c and z_a are cation and anion formal charge. These relationships may lead to predictions of structural variation with temperature, pressure, and composition. Furthermore, in compounds with structures that have geometrical limits, phase equilibria may be predicted.

Zusammenfassung: Die Arbeit gibt einen Überblick über Strukturbestimmungen bei erhöhten Temperaturen und Drücken. Einkristall-Röntgenapparaturen sind jetzt mit Temperaturen bis 1100 °C und Drücken bis 100 kbar belastbar. Eine beheizte Einkristall-Diamantstempel-Zelle hat 450 °C bei 30 kbar erreicht. Ein bedeutender Teil der PT-Bedingungen in Kruste und oberem Mantel ist daher für Einkristall-Experimente zugänglich.

Die mittlere lineare thermische Ausdehnung. α_{poly}, und die Kompressibilität, β_{poly}, jedes Typs von Kation-Anion-Polyedern sind unabhängig vom Strukturtyp. Einfache, empirische Beziehungen erlauben die Vorhersage von α_{poly} und β_{poly} aus ionischen Bindungsparametern:

---

* Abstracted from R. M. Hazen & L. W. Finger (1982, in press): Comparative Crystal Chemistry: The Variation of Crystal Structure with Temperature, Pressure, and Composition. – Wiley International, New York/London.

$$\alpha_{poly} = 4.0\,(4) \times 10^{-6} \frac{n}{S^2 z_c \cdot z_a}\ °C^{-1},$$

und

$$\beta_{poly} = 0.133\,(4)\ (\bar{d}^3/S^2 z_c \cdot z_a)\ Mbar^{-1},$$

wobei n = Koordinationszahl, d = mittlerer Kation-Anion-Abstand, S = Ionizitätsterm, z_c = formale Ladung des Kations und z_a = formale Ladung des Anions. Diese Beziehungen können zu Vorhersagen der strukturellen Veränderungen mit der Temperatur, dem Druck und der Zusammensetzung führen. Weiter können bei Strukturen mit geometrischen Grenzen Phasengleichgewichte vorhergesagt werden.

1. Introduction

In 1912 Von Laue discovered the diffraction of X-rays by crystals and thus revolutionized the solid-state sciences. His observations demonstrated the periodicity of atoms and the approximate dimension of those repeats. Methods that used positions and intensities of diffracted X-rays to infer crystal structure were soon developed. For forty years virtually all X-ray crystallographers applied these techniques to the solution of new crystal structures. By the mid-1950's most common types of inorganic structures had been solved.

As more and more crystal structures were resolved the objectives of many crystallographers gradually changed. Studies of atomic arrangements were replaced by more detailed investigations of chemical bonding and electron distribution. One common approach to these studies of bonding was the determination of the small structural differences between isomorphous compounds. In many isomorphous materials and their solid solutions the subtle variations in atomic parameters within a given topology were related to the differing electronic structures of the substituting atoms. Such *comparative* crystallographic investigations led directly to important concepts of crystal chemistry, including the periodicity of ionic radii, the effects of radius ratio on coordination number, and geometrical limits of certain atomic topologies (Pauling, 1960).

Another obvious, but technologically more difficult, problem in comparative crystallography is the nature of the subtle atomic positional and lattice variations that are manifest in thermal expansion and compression. In general, the structural response to changes in temperature or pressure, as with changes in composition, is not a simple scaling of the unit cell. Complete three-dimensional structure refinements at several temperatures and pressures are required to elucidate these changes. The resulting "structural equations of state" are well worth the effort for they provide important data on both theoretical and applied problems in solid-state sciences.

Empirical relationships that lead to predictions of structural variation with temperature, pressure, and composition are important in modeling the behavior of materials under conditions not yet studied or attainable in the laboratory. An empirical knowledge of ionic radii, for example, has led to the synthesis of numerous economically valuable analogs of natural compounds. Similarly, empirical models of the variation of structure with temperature and pressure can be used to predict material properties such as molar volume or crystal-field energies at high temperatures and pressures (for example, under conditions in the earth's mantle). Furthermore, if a phase transition is known to be controlled by structural parameters, then phase stability can be deduced from the predicted structure at specific temperatures, pressures, and compositions.

In spite of the theoretical and empirical significance of comparative crystallographic studies, technological problems entailed in these experiments have been solved only recently. The collection of multiple, precise data sets for comparative purposes was not practical prior

to the development of automated single-crystal diffractometer systems. These systems, combined with the arsenal of crystallographic software and high-speed computers, result in the rapid automated completion of tasks that would have required several months two decades ago. Another vital technological advance has been the development of small, stable resistance heaters and diamond-anvil pressure cells in which single crystals can be maintained in a stable orientation at constant high temperature and pressure during X-ray experiments lasting several days. The solution of these formidable technological problems, and the application of this technology to geological problems, are the subject of this review.

2. High-temperature crystallography

The determination of crystal structures at high temperatures is of fundamental importance to studies of the solid state. It is not surprising, therefore, that high-temperature devices were applied to X-ray cameras by the 1930's, shortly after the development of powder X-ray diffraction as a useful identification technique. Although many heaters for powders were in use, there was still no simple and effective heater for single crystals when Goldschmidt (1964) prepared his comprehensive *Bibliography of High-Temperature X-ray Diffraction Techniques*. One of the first practical single-crystal heaters for X-ray diffraction was introduced by Foit & Peacor (1967), who designed their device to accommodate Weissenberg geometry. The heater was not easily adapted to automated systems or to other diffraction configurations and therefore did not receive widespread use. Several other heaters were described shortly thereafter, and by the mid-1970's high-temperature crystal structures were being determined in several laboratories (e. g., Prewitt, 1976).

2.1 Types of heaters

Three types of single-crystal heaters have been employed in crystallographic studies: open-flame, gas-flow, and radiative. Smyth (1969) employed an open-flame oxy-hydrogen torch in his experiments on $(Mg_{0.3}Fe_{0.7})SiO_3$ clinopyroxene. An obvious advantage of this device is that extremely high temperatures, greater than 1500 °C, may be generated. The open-flame heater is severely limited, however, in that temperature at the crystal is stable to only about ± 100 °C owing to minor fluctuations in gas flow and air convection.

Furnaces developed by Prewitt et al. (1970) and Smyth (1972) rely on a hot gas, usually nitrogen, to heat the single crystal. The basic features common to these heaters are a coiled resistance heating element of noble metal wire and a central channel through which high-purity nitrogen gas is directed over the crystal. Some designs also have water-cooling to reduce heating of diffraction apparatus. Gasflow heaters have proven sucessful in producing and maintaining stable (± 2 °C in some designs) high temperatures to 900 °C for several days and have thus been employed in more than a dozen high-temperature structure studies. A significant limitation of the technique is that temperatures above 900 °C have not been attained. Furthermore, the gas and water lines are cumbersome, and temperature may fluctuate if fluid flow rates are not constant. For these reasons gas-flow crystal heaters have been largely supplanted by radiative designs.

The most versatile heaters for single crystals available today are based on the design developed at the State University of New York at Stony Brook by Brown et al. (1973). In the original design a miniature resistance heating element in the shape of a horseshoe was placed around the crystal. Temperatures in excess of 1100 °C have been obtained with relatively low power requirements, and no gas or water lines are required. Furthermore, the small size and

wide angular access to the crystal facilitate the adaptation of this device to different X-ray diffraction configurations.

2.2 Crystal mounting

Successful high-temperature crystallography is dependent on a stable crystal mount. Some highly refractory compounds, such as magnesium silicates, may be attached directly to the join bead of a thermocouple. Platinum becomes an adhesive when heated to incandescence, and a strong bond between crystal and thermocouple may thus be achieved. An advantage of this mounting procedure is its simplicity, though its use is limited to the relatively few compounds that do not alter at high temperature in air. A possible disadvantage is that the thermocouple EMF vs. temperature profile may be altered by the presence of a crystal adhering to the join bead, thus adding uncertainty to the temperature calibration.

By far the most widely used mount in high-temperature crystallography is the silica glass capillary. The single crystal is placed at the sealed end of a capillary with inner diameter slightly larger than the crystal diameter. The crystal is then wedged against the end of the capillary by insertion of a silica glass needle, with mullite wool if needed. Crystals subject to oxidation at high temperature (for example, compounds of Fe^{2+} or Mn^{2+}) must be isolated from the atmosphere, and an evacuated silica capillary mount is then used.

2.3 Temperature calibration

Successful high-temperature crystallography is dependent upon accurate temperature calibration. All calibration procedures currently in use rely on a sensing thermocouple; the configuration and details of measurement, however, differ widely. A common thermocouple configuration in high-temperature work is a Pt-$Pt_{90}Rh_{10}$ bead adjacent to, but outside, the silica glass capillary. The EMF of this thermocouple may read out directly on a recorder, or it may be used in a feedback system to regulate power to the furnace. In general, the temperature at the thermocouple will not be the same as the crystal inside the capillary, so careful calibration experiments are required. Furthermore, each individual thermocouple differs owing to the size and interface geometry of the join bead. Each thermocouple should therefore be calibrated against fixed-point standards in the appropriate experimental configuration before data are collected.

Use of an internal calibrant may result in accurate temperature determination, independent of thermocouple measurements. A single crystal of a cubic material with a precisely determined thermal expansion coefficient could be included in the glass capillary adjacent to the single crystal under investigation. A single lattice-parameter measurement on the standard cubic crystal is sufficient to define temperature; if the unit-cell edge of sodium chloride is measured to 1 part in 10,000 (the normal precision), then temperature is defined to within 0.7 °C. Furthermore, systematic errors in thermocouple calibration are eliminated with this internal calibration technique.

2.4 Future prospects

Few advances in heater design have appeared since the work of Brown et al. (1973). The lack of new developments may be in large part due to the vast number of crystallographic problems yet to be studied in the temperature range below 1100 °C, though the present capabilities may also reflect the absolute limits of radiative heating with Pt-wire heaters.

Should higher temperatures be required other heating techniques may prove necessary. In addition to the open-flame procedures mentioned above, laser heating of single crystals may

hold promise for generating very high temperatures. As with flame heaters, however, it is difficult at present to maintain constant uniform temperatures with lasers.

3. High-pressure crystallography

3.1 Diamond-anvil pressure cells

Diamond is remarkable both because it is the hardest known material and because it is transparent to many ranges of electromagnetic radiation. These attributes of diamond have led to its widespread use in the generation of high pressure in studies of the physical properties of matter.

The idea of an opposed-diamond configuration for generating high pressure (Fig. 1) was developed independently and nearly simultaneously by workers at the National Bureau of Standards (Weir et al., 1959) and the University of Chicago (Jamieson et al., 1959). In their earliest experiments the NBS group used the diamond cell as an optical window on the high-pressure environment, viewing samples in transmitted light, whereas workers at Chicago concentrated on powder X-ray diffraction techniques with the X-ray source parallel to the diamond anvil faces. Both groups, however, employed the opposed-diamond configuration, which permits the generation of high pressures at the diamond interface with comparatively little force, and which is now the basic element of almost all diamond cells.

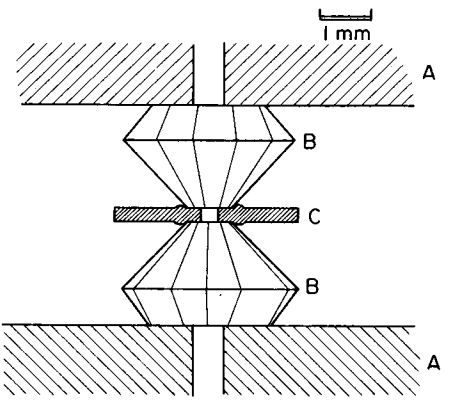

Fig. 1. Opposed-diamond configuration for high-pressure, single-crystal experiments. All such devices have diamond supports (A), two diamond anvils (B), and a metal foil gasket (C).

In its original form the opposed-diamond cell was not suitable for single-crystal X-ray diffraction because crystals would be crushed between the anvil faces. An important development, therefore, was Van Valkenburg's (1964) metal-foil gasketing technique, in which a thin metal sheet with a hole smaller than the diamond anvil faces was placed between the diamonds to act as a sample chamber (Fig. 1). The gasket was originally designed for study of the crystallization of fluids at high pressure, and the first high-pressure, single-crystal X-ray experiments were performed on Ice VI in a gasketed diamond cell (Block et al., 1965; Weir et al., 1965). The NBS reseachers also recognized that the gasketing procedure could be used to enclose a single crystal in a hydrostatic environment. Experiments on high-pressure phases of potassium nitrate (Weir et al., 1969a) and on elemental cesium and gallium (Weir et al., 1971) demonstrated the usefulness of this approach.

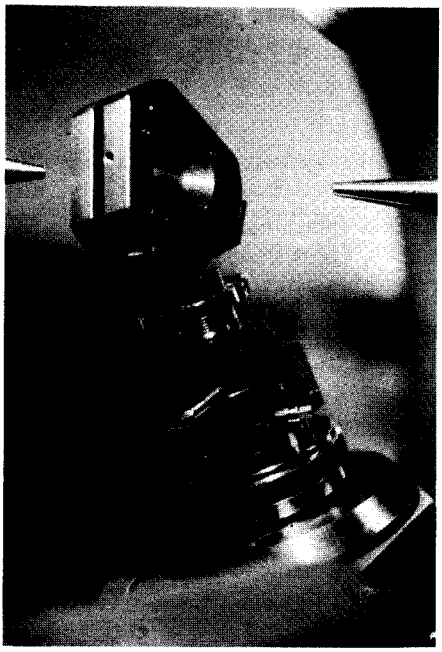

Fig. 2. Goniometer head, cradle, and pressure cell for single-crystal X-ray diffraction (from Hazen & Finger, 1977b).

All the pioneering NBS single-crystal work was performed with a specially modified Buerger precession camera (Weir et al., 1969a) with a lever-arm pressure cell made entirely of beryllium, except for the gasket and diamond components. This diamond cell was too large to be easily adapted to standard X-ray equipment. These early contributions, therefore, included only high-pressure unit-cell dimensions and space groups and did not present complete structure refinements based on integrated intensity data. Merrill & Bassett (1974) applied the opposed-diamond principle in their construction of a miniature diamond cell for single-crystal X-ray diffraction (Fig. 2). This cell, simple in construction and use, is small enough to be adaptable to most standard single-crystal X-ray cameras and diffractometers. The first complete three-dimensional structure refinements of crystals at high pressure were performed on $CaCO_3$ (calcite; Merrill & Bassett, 1975) and $BaFeSi_4O_{10}$ (gillespite; Hazen & Burnham, 1974) with the Merrill & Bassett cell.

Several other single-crystal, diamond-anvil pressure cells have been introduced in recent years. Keller & Holzapfel (1977) of Stuttgart designed a single-crystal X-ray cell with accessibility to reciprocal space similar to that of the Merrill & Bassett cell, but with improved diamond alignment and a more uniform loading mechanism, resulting in pressure generation to about 100 kbar. This Stuttgart cell is significantly more massive than the miniature design, as well as far more complex in construction. The added pressure range available with this design must be weighed against the increased expense and operating difficulties.

Schiferl (1977) continued the tradition of early workers at the University of Chicago by designing a diamond cell with transverse X-ray configuration. This design, unique among single-crystal cells, has the advantage of accessibility to nearly half of the Ewald sphere. High-angle diffraction positions can be measured, for example, resulting in increased precision in lattice-constant measurements. The Schiferl cell has been used at pressures to approximately 100 kbar. Although the cell provides excellent access for unit-cell determinations, the trans-

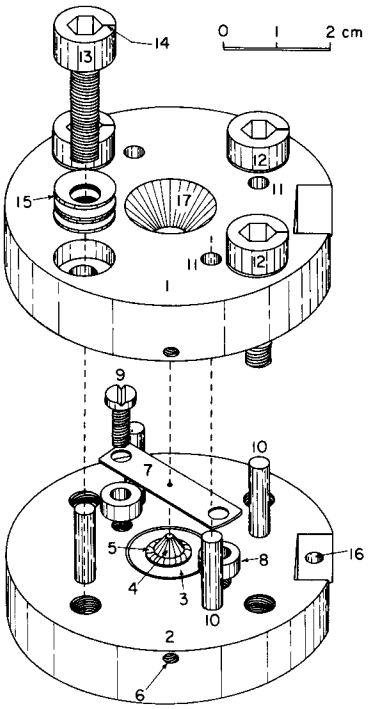

Fig. 3. Modified diamond-window, high-pressure cell for study of single crystals of solidified gases. Parts: 1, 2, end plates; 3, Be support disks; 4, diamond anvils; 5, epoxy cement; 6, set screws for adjusting part 3; 7, gasket; 8, spacers; 9, screw; 10, positioners; 11, hole for positioners; 12, 13, screws for raising sample pressure; 14, groove; 15, Belleville springs; 16, mounting notch (Mao & Bell, 1980).

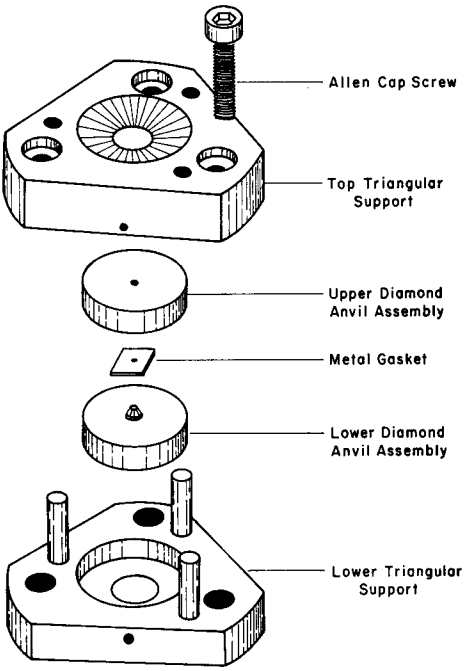

Fig. 4. Assembly of the Merrill & Bassett (1974) diamond-anvil cell, as modified by Hazen & Finger (1977b).

verse configuration is not well suited for integrated intensity measurements. This limitation is a consequence of the very complex absorption paths owing to X-rays passing through the side of a diamond, gasket, thin crystal, and back through the diamond, as compared with the simple radial symmetry of absorption in transmission mode experiments.

Mao & Bell (1980) constructed a diamond-anvil cell for the study of single crystals of materials that are normally gases under ambient conditions. The cell is similar in principle to the Merrill & Bassett (1974) design, though extensive modifications are involved. The cell has four load-bearing screws, rather than the three-screw configuration of the Merrill & Bassett pressure device (Fig. 3). Loading of a liquefied sample under cryogenic conditions is accomplished in a dewar, and the cell is closed and pressure-sealed remotely.

3.2 Operation of the diamond cell

Assembly of the Merril & Bassett pressure cell is illustrated in Fig. 4. Details of the construction and use of the cell are presented by Hazen & Finger (1982). There are five main

components of the cell. Triangular steel supports are machined from stainless steel. Beryllium disks, which are transparent to MoKα X-rays, act as diamond supports. Diamonds are 1/10 carat gemstones (less expensive yellow diamonds may be used) cut with anvil faces 0.6 to 1.0 mm diameter. The gasket is sheet metal, usually a hardened steel or nickel alloy, ~ 250 μm thick, with a 300-μm-diameter hole. The two halves of the cell are held together, and pressure is applied by three screws, which are hand-tightened.

Crystal mounting is accomplished by placing the gasket against one diamond anvil and loading the sample chamber (i. e., the gasket hole) with the single crystal, chips of ruby, and a pressure fluid. The crystal position is fixed by a small amount of petroleum jelly, which acts as a glue. A 4:1 by volume mixture of methanol : ethanol has been found to be an effective hydrostatic pressure transmitting fluid to approximately 100 kbar (Piermarini et al., 1973). The ruby chips serve as an internal pressure standard, based on the wavelength shift of the R_1 fluorescence line (Forman et al., 1972; Piermarini et al., 1975; Mao & Bell, 1976).

The Merrill & Bassett cell is mounted on a modified goniometer head (Fig. 2) and is easily adapted to precession cameras and diffractometers. Molybdenum (MoKα) radiation is the best source for diamond-cell work because of its penetrating wavelength and intrinsic bright-

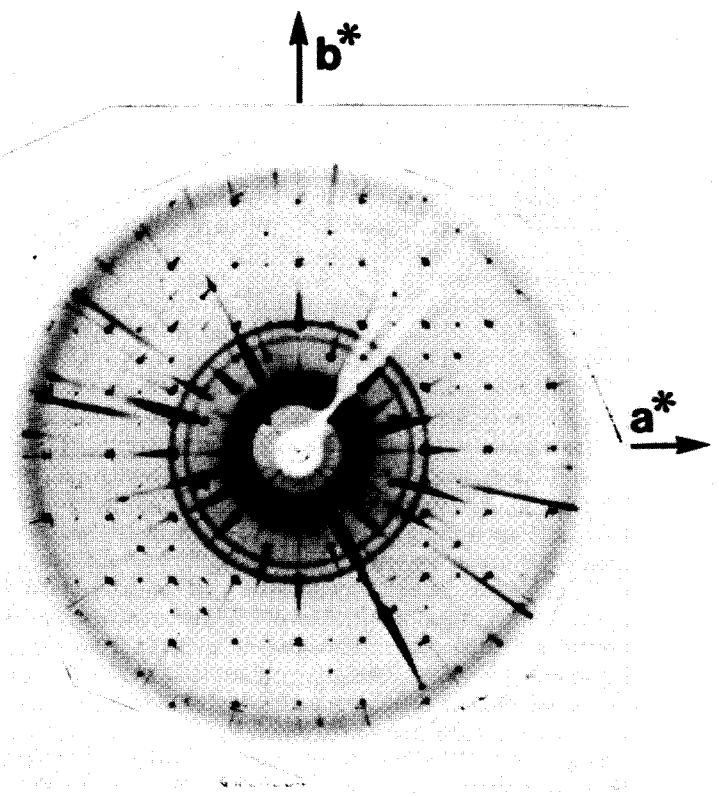

Fig. 5. Precession photograph of gillespite ($BaFeSi_4O_{10}$) at 12 kbar. Visible on the photograph are beryllium powder rings, intense diamond streaks, and sharp spots from gillespite in the (001) tetragonal orientation. Taken with Zr-filtered Mo radiation; exposure 24 hours at 40 kV and 16 mA.

ness. Monochromated X-radiation is not essential, though it enhances peak-to-background ratios. A typical precession photograph is illustrated in Fig. 5. Beryllium powder rings and strong diamond streaks are observed in addition to the sharp spots of the single crystal under study.

Procedures for high-pressure diffractometry have been reviewed by Finger & King (1978) and King & Finger (1979). Two important changes in operational procedures from room-condition intensity measurements are required. First, an absorption correction for diamond and beryllium components of the pressure cell must be applied. This correction is straightforward for the radially symmetric Merrill & Bassett cell. Second, the diffractometer should be operated in the "fixed-Ø" mode to optimize access to reciprocal space (Finger & King, 1978).

3.3 Future prospects

Improvements in pressure calibration and an increased hydrostatic pressure range are two important directions for future work. One possible solution to both problems is the use of a gas such as argon as *both* pressure medium and internal standard. Hazen et al. (1980) observed that argon at 20 °C crystallizes above 12 kbar to a highly compressible crystalline solid, which always forms single crystals in the diamond cell. Argon is soft enough to provide a hydrostatic environment for the single crystal under study, and the change in the cubic cell edge of argon is sufficiently large that it may be used to define pressure to within ± 10 bar, nearly fifty times more precise than the ruby calibration.

4. High-temperature, high-pressure crystallography

The previous sections have dealt with crystallographic studies at high temperature or high pressure alone. Pressure and temperature must be combined, however, if comprehensive equation-of-state data are to be obtained. Crystallography at high temperature and pressure presents formidable challenges, both in design and calibration, and much of this technology is still in the developmental stage.

4.1 Heating the diamond cell

An obvious solution to the problem of subjecting a single crystal to simultaneous high temperature and high pressure is to heat the diamond-anvil cell. Consequently, diamond cells were heated almost from the beginning of their development. The simplest procedure for heating a diamond cell was used at the National Bureau of Standards, where a cell with pressurized sample was placed on a hot plate and warmed to a maximum temperature of more than 200 °C. The cell was then transferred to a microscope where the high-temperature, high-pressure behavior of the sample was observed during cooling (A. Van Valkenburg, pers. comm.).

Resistance heaters, with wire windings placed around the diamond and sample region, have been widely used to provide uniform temperatures for long time periods. The temperature of the diamond cell is limited to no greater than 1000 °C owing to graphitization of the diamonds. Furthermore, gasketing materials now in use become too weak to support high pressures at temperatures above 800 °C, placing an additional restriction on the temperature range. Yet another constraint is that an inert atmosphere is required above 700 °C to avoid oxidation of diamonds.

A variety of resistance-furnace configurations have been attempted. Several designs incorporate a winding 2 to 4 cm in diameter, which heats both diamonds and supports (Van

Valkenburg, 1963; Bassett & Takahashi, 1965; Fourme, 1968; Barnett et al., 1973). In these diamond cells the sample is heated while the pressure-loading mechanism remains relatively cool. Bassett & Ming (1972) used a novel long and narrow cell that fits into a standard tube furnace. The spring remains cool outside the furnace, while pressure is applied to the diamond anvils via a long piston. Recent designs by Sung (1976) and Hazen & Finger (1981) incorporate a miniature winding 4 to 6 mm in diameter that heats the diamond and sample area of a small cell (see below).

Moore et al. (1970) used the gasket as the resistance element. This device was not used above 300 °C because of the rapid conduction of heat away from the sample chamber by diamond, which is one of the most efficient thermal conductors.

Lasers provide a method of heating samples to temperatures significantly greater than the decomposition point of diamond. Bassett & Ming (1972) and Ming & Bassett (1974) achieved steady-state temperatures to 2000 °C and pulsed temperatures of 3000 °C in polycrystalline samples at pressures greater than 200 kbar with a YAG laser. High temperatures are attainable because a sample that absorbs laser energy, or is mixed with an absorber, may be heated to several thousand degrees Centigrade while the transparent diamonds remain relatively cool because of their high thermal conductivity. An obvious difficulty of this technique is that high thermal gradients are produced in the sample chamber making calibration of temperature and pressure difficult. In addition, though lasers are ideal for heating polycrystalline samples in experiments where the diamond-cell orientation is constant, cell orientation in single-crystal X-ray experiments must be varied, rendering constant heating of a laser-irradiated sample difficult. For these reasons laser heating has not yet been adopted in single-crystal, diamond-cell experiments.

4.2 Single-crystal X-ray studies

Hazen & Finger (1981) added a miniature resistance heater to the Merrill & Bassett diamond cell for high-temperature, high-pressure studies of single crystals (Fig. 6). They produced the first high-T, high-P, three-dimensional crystal structure using this device. The design and operation of this "PT cell" are similar to those of the high-pressure cell, except for the following important changes.

Beryllium disks are replaced by boron carbide components owing to the softening of Be at high temperature. It is difficult to machine holes in boron carbide, and the prototype PT cells had no optical access. Pyrophyllite and mica insulating pieces are added to the cell to concentrate heat at the sample. The three screws are partly isolated from the body of the PT cell by using Belleville spring washers (Fig. 6).

The miniature heater employs the design of Ohashi & Hadidiacos (1976) in which the furnace winding is half platinum and half $Pt_{90}Rh_{10}$ thermocouple wire, with a join bead at the center of the winding. Power is supplied to the furnace during half a cycle of AC current, and the EMF of the thermocouple is sensed during the other half and is used to regulate the power to the heater.

Calibration of temperature is accomplished by comparing heater EMF to the temperature of a single crystal (based on crystal thermal expansion) at room pressure in the proper experimental configuration. Pressure is then calibrated in any experiment by measuring the cell edge of a cubic internal standard crystal (usually CaF_2) at the known temperature (Hazen & Finger, 1982). Maximum conditions thus far produced are 450 °C and 30 kbar; complete structure refinements of the mineral diopside at 375 °C and 20 kbar required 7 days of continuous heating during data collection.

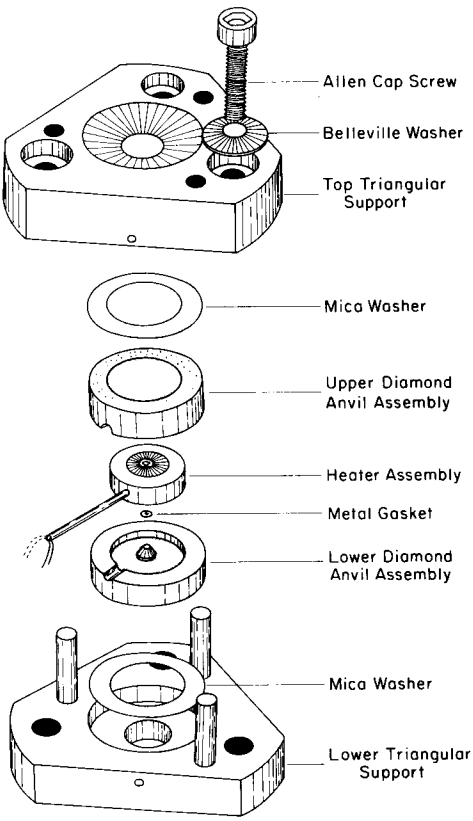

Fig. 6. Exploded view of the high-temperature, high-pressure, diamond-anvil cell (from Hazen & Finger, 1981).

4.3 Future prospects

High-temperature, high-pressure crystallography is in its infancy. Thousands of exciting problems, from phase transition studies to P-T-V systematics, are now practical. Improvements in the range of conditions available to the PT cell will surely be made in the coming years, and more problems of significance to geology will thus be accessible for study.

5. Structural variations with temperature

5.1 Bond expansion data

In the previous three sections it has been demonstrated that crystal structures can be determined on material under nonambient conditions. Results of studies of single-crystal structures at high temperatures and high pressures are reviewed in the following sections. Data are presented in terms of the variation of cation-anion bond distances within polyhedra. Information on the variation of structural dimensions with temperature or pressure comes from two distinct types of studies. Complete three-dimensional structure refinements are the

Table 1. Complete three-dimensional, high-temperature (> 400 °C), single-crystal structure refinements.*

Mineral name	Formula	Structure type	Reference
Periclase	MgO	Rock salt	Hazen (1976 a)
Karelianite	V_2O_3	Corundum	Robinson (1975)
—	Ti_2O_3	Corundum	Rice & Robinson (1977)
Cristobalite	SiO_2	Cristobalite	Peacor (1973)
—	$PbTiO_3$	Perovskite	Glazer & Mabud (1978)**
—	$Ba_2Bi^{3+}Bi^{5+}O_6$	Perovskite	Cox & Sleight (1979)
Rutile	TiO_2	Rutile	Meagher & Lager (1979)
Brookite	TiO_2	Brookite	Meagher & Lager (1979)
Anatase	TiO_2	Anatase	Horn et al. (1972)
Armalcolite	$(Fe,Mg)Ti_2O_5$	Pseudobrookite	Wechsler (1977)
Sillimanite	Al_2SiO_5	Sillimanite	Winter & Ghose (1979)
Andalusite	Al_2SiO_5	Andalusite	Winter & Ghose (1979)
Kyanite	Al_2SiO_5	Kyanite	Winter & Ghose (1979)
β-Eucryptite	$LiAlSiO_4$	Stuffed quartz	Pillars & Peacor (1973)
High-Albite	$NaAlSi_3O_8$	Feldspar	Prewitt et al. (1976)
High-Albite	$NaAlSi_3O_8$	Feldspar	Winter et al. (1979)
Low Albite	$NaAlSi_3O_8$	Feldspar	Winter et al. (1977)
Anorthite	$CaAl_2Si_2O_8$	Feldspar	Foit & Peacor (1973)
Nepheline	$(Na,Ca,K)_8Al_8Si_8O_{32}$	Nepheline	Forman & Peacor (1970)
Natrolite	$Na_2Al_2Si_3O_{10} \cdot 2H_2O$	Zeolite	Peacor (1973)
Cordierite	$Mg_2Al_2Si_5O_{18} \cdot (H_2O)_x$	Cordierite	Hochella et al. (1979)
Phlogopite	$KMg_3AlSi_3O_{10}F_2$	Mica	Takeda & Morosin (1975)
Sphene	$CaTiSiO_5$	Sphene	Taylor & Brown (1976)
—	Ni_2SiO_4	Spinel	Finger et al. (1979)
Pyrope	$Mg_3Al_2Si_3O_{12}$	Garnet	Meagher (1975)
Grossular	$Ca_3Al_2Si_3O_{12}$	Garnet	Meagher (1975)
Forsterite	Mg_2SiO_4	Olivine	Hazen (1976 b)
Hortonolite	$(Mg,Fe)_2SiO_4$	Olivine	Brown & Prewitt (1973)
Ferro-hortonolite	$(Fe,Mg)_2SiO_4$	Olivine	Smyth & Hazen (1973)
Fayalite	Fe_2SiO_4	Olivine	Smyth (1975)
—	Ni_2SiO_4	Olivine	Lager & Meagher (1978)
Monticellite	$CaMgSiO_4$	Olivine	Lager & Meagher (1978)
Glauchochroite	$CaMnSiO_4$	Olivine	Lager & Meagher (1978)
Protoenstatite	$MgSiO_3$	Orthopyroxene	Smyth (1971)
Orthoferrosilite	$FeSiO_3$	Orthopyroxene	Sueno et al. (1976)
Ferrohypersthene	$(Fe,Mg)SiO_3$	Orthopyroxene	Smyth (1973)
Clinohypersthene	$(Fe,Mg)SiO_3$	Clinopyroxene	Smyth & Burnham (1972) Smyth (1974)
Spodumene	$LiAlSi_2O_6$	Clinopyroxene	Cameron et al. (1973)
Acmite	$NaFe^{3+}Si_2O_6$	Clinopyroxene	Cameron et al. (1973)
Jadeite	$NaAlSi_2O_6$	Clinopyroxene	Cameron et al. (1973)
Ureyite	$NaCrSi_2O_6$	Clinopyroxene	Cameron et al. (1973)
Hedenbergite	$CaFeSi_2O_6$	Clinopyroxene	Cameron et al. (1973)
Diopside	$CaMgSi_2O_6$	Clinopyroxene	Cameron et al. (1973)
Diopside	$CaMgSi_2O_6$	Clinopyroxene	Finger & Ohashi (1976)
Cummingtonite	$Mg_7Si_8O_{22}(OH)_2$	Amphibole	Sueno et al. (1972)
Tremolite	$Ca_2Mg_5Si_8O_{22}(OH)_2$	Amphibole	Sueno et al. (1973)

* The numerous high-temperature, single-crystal X-ray studies that do not contain structure refinements are not included, even though structural inferences may be made from them.

** High-temperature powder profile refinement.

most obvious sources of data, but it is also possible to derive this information from unit-cell dimensions alone in many constrained or simple structures. The structures of NaCl, CsCl, CaF_2, and cubic ZnS are all fixed in that there are no variable positional parameters. Thermal expansion data on materials that crystallize in these structures thus provide information on bond thermal expansion as well. Other simple structures, including those of rutile (TiO_2), corundum (Al_2O_3), hexagonal ZnS, and ZrO_2, also have bulk expansions that are similar to expansions of cation-anion bonds.

Several dozen studies of structures at high temperature (Table 1) provide a wealth of data on the variation of cation-anion (primarily cation-oxygen) bonds with temperature. From these high-temperature studies it is possible to calculate linear expansion coefficients, α_l, for individual cation-anion bond distances, d, and the mean linear expansion coefficient, $\bar{\alpha}_l \equiv \alpha_{poly}$, for the average bond length, $\bar{d}$, of all cation-anion bonds within a given polyhedron:

$$\alpha_l = \frac{1}{d}\left(\frac{\Delta d}{\Delta T}\right), \tag{1}$$

$$\bar{\alpha}_l = \frac{1}{\bar{d}}\left(\frac{\Delta \bar{d}}{\Delta T}\right). \tag{2}$$

Polyhedral volume thermal expansion, $\bar{\alpha}_v$, is defined as

$$\bar{\alpha}_v = \frac{1}{V_p}\left(\frac{\Delta V_p}{\Delta T}\right) \approx 3\bar{\alpha}_l. \tag{3}$$

Eq. 3 is valid only if polyhedral distortions are approximately constant with temperature. Observed distortion parameters of tetrahedral and octahedral sites vary little with temperature.

5.2 Empirical bond distance-temperature relationships

Several attempts have been made by previous investigators to relate thermal expansion to bonding parameters or other physical properties. Megaw (1938) proposed that in crystals with only one type of bond (homodesmic crystals) thermal expansion is a function of Pauling bond strength (defined as z/n, where z and n are cation charge and coordination number, respectively). She proposed the relationship

$$\alpha \propto n^2/z^2. \tag{4}$$

This equation is in agreement with the observed thermal expansion of many simple compounds, but it fails for many of the more complex compounds listed in Table 1.

In a more recent study of pyroxene crystal structures at high temperature, Cameron et al. (1973) related expansion coefficients of metal-oxygen bonds to bond strengths (defined as $4\nu^2\pi^2\mu c^2$, where ν is M–O stretching frequency, μ is reduced mass, and c is the velocity of light). Although their relationship closely represents the bond expansions of their study, the Cameron et al. equation does not predict bond expansion in many other types of silicates.

Hazen & Prewitt (1977) tabulated $\bar{\alpha}_l$ for several dozen cation-oxygen polyhedra. Their first important observation is that all cation coordination polyhedra of a given type (i. e., all magnesium-oxygen octahedra or silicon-oxygen tetrahedra) demonstrate similar expansion coefficients. For example, all Mg octahedra studied (18 different polyhedra in 10 compounds) have $\bar{\alpha}_l = 14 \times 10^{-6}\ °C^{-1}$ within one estimated standard deviation (Fig. 7). Similar behavior is observed for other polyhedra as well.

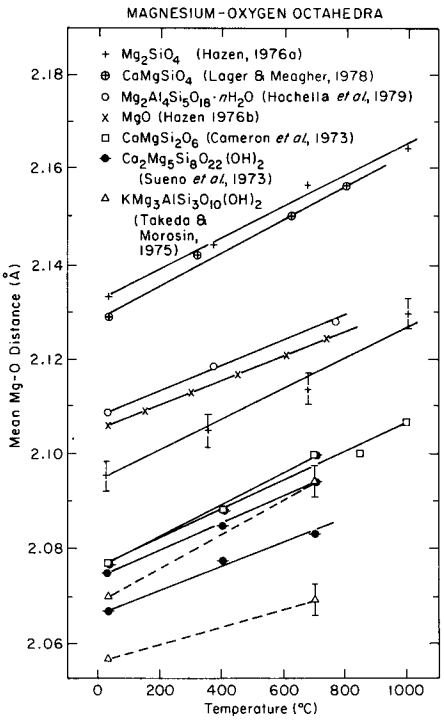

Fig. 7. Variation of average Mg–O bond distances in magnesium-oxygen octahedra vs. temperature.

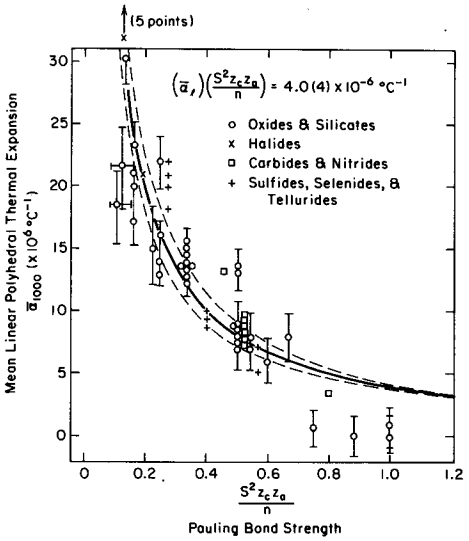

Fig. 8. The inverse relationship between polyhedral thermal expansion and Pauling bond strength.

An important generalization stemming from these observations is that the thermal expansion coefficient for each type of polyhedron is *independent of structural linkages* of the polyhedron, providing the site composition and topology of the structure do not change with temperature. Thus, for each type of cation-oxygen polyhedron there exists a value for an expansion coefficient that may be used to predict behavior at high temperature. A second generalization is that all oxygen-based polyhedra with the same Pauling bond strength (cation charge divided by coordination number) have the same $\bar{\alpha}_l$. For example, octahedra of Ni, Mg, Co, Fe^{2+}, Cd, Mn^{2+}, Ca, Ba, and Sr *all* have $\bar{\alpha}_l$ of $14 \pm 1 \times 10^{-6}\ °C^{-1}$. This fact is remarkable given the range of atomic masses and size represented by these cations.

A plot of Pauling bond strength vs. $\bar{\alpha}_l$ (Fig. 8) reveals a simple inverse relationship between the two parameters:

$$(\bar{\alpha}_l)\ \frac{S^2 z_c z_a}{n} = 4.0(4) \times 10^{-6}\,°C^{-1}, \qquad (5)$$

where S^2 is an ionicity factor (Hazen & Finger, 1979a) *defined* to be 0.50 for all oxides and silicates, and *observed* to be 0.75 for all halides, 0.40 for chalcogenides, 0.25 for phosphides and arsenides, and 0.20 for nitrides and carbides. (Bond compression data are used to derive S^2 values, as discussed in the next section.)

Eq. 5 is physically reasonable. If bond strength is zero between two atoms, as in an inert gas, then thermal expansion is infinite. If bond strength is very large, then thermal expansion

approaches zero. In practice eq. 5 may be used to predict the thermal expansion coefficient of most polyhedra to within 15 %. The formula does not work well for very large alkali sites, for which the coordination number may not be well defined owing to site distortions. The formula is also inadequate for strong bonds ($z_c/n \geq 0.75$), which are observed to have expansion coefficients less than those predicted by eq. 5. Yet another limitation of this bond strength-thermal expansion relationship is the lack of information on thermal corrections to bond distances. Nevertheless, it is possible to predict relative values of polyhedral thermal expansion and in many cases quantitative expansion information can also be predicted.

6. Structural variations with pressure

6.1 Bond compression data

Bond compressibility, β, is defined in a way analogous to the bond expansion coefficient:

$$\beta_l = \frac{-1}{d}\left(\frac{\Delta d}{\Delta P}\right) \text{ and } \overline{\beta_l} = \frac{-1}{\bar{d}}\left(\frac{\Delta \bar{d}}{\Delta P}\right). \tag{6}$$

Polyhedral volume compressibility, $\beta_{poly} \equiv \overline{\beta_v}$, is given by

$$\overline{\beta_v} \approx 3\,\overline{\beta_l}. \tag{7}$$

Yet another important definition is the bulk modulus, K, which is the inverse of volume compressibility (e. g., $K_{poly} = 1/\beta_{poly}$).

Bond compression data, like expansion data, are derived both from fixed-structure compressibilities and from complete structure refinement of more complex crystals at high pressure (Table 2). Hazen & Finger (1979 a) have tabulated these high-pressure data for more than 100 cation-anion polyhedra in oxides, halides, chalcogenides, and other compounds.

6.2 Empirical bond distance-pressure relationships

Percy Bridgman was one of the first to attempt an empirical expression for the prediction of crystal bulk moduli. In his classic study of 30 metals, Bridgman (1923) found that compressibility was proportional to the 4/3 power of molar volume. The importance of mineral bulk moduli in modeling the solid earth led Orson Anderson and his coworkers (Anderson & Nafe, 1965; Anderson & Anderson, 1970; Anderson , 1972) to expand Bridgman's treatment of oxygen-based, mineral-like compounds. For isostructural materials, it is found that compressibility is proportional to molar volume or, as expressed in Anderson's papers:

(bulk modulus) × (molar volume) = constant.

Although this relationships is empirical, theoretical arguments in suport of the KV trend may be derived from a simple two-term bonding potential expression.

The same theoretical arguments used to explain the observed KV relationship in isostructural compunds may be used to predict a bulk modulus-volume relationship for cation coordination polyhedra. Hazen & Prewitt (1977) found such an empirical trend in cation polyhedra from oxides and silicates:

$$\frac{K_{poly}\bar{d}^3}{z_c} = \text{constant}, \tag{8}$$

where z_c is the cation formal charge and $\bar{d}$ is the cation-anion mean bond distance.

Table 2. Complete three-dimensional, high-pressure (> 10 kbar), single-crystal, structure refinements.*

Mineral name	Formula	Structure type	Reference
Antimony	Sb	Arsenic	Schiferl (1977)
Selenium	Se	Selenium	Keller et al. (1977)
Tellurium	Te	Selenium	Keller et al. (1977)
Periclase	MgO	Rock salt	Hazen (1976 a)
Halite	NaCl	Rock salt	Finger & King (1978)
Troilite	FeS	Nickel arsenide	King (1978)
Ruby	Al_2O_3	Corundum	Finger & Hazen (1978)
Ruby	Al_2O_3	Corundum	d'Amour et al. (1978)
Hematite	Fe_2O_3	Corundum	Finger & Hazen (1980)
Eskolaite	Cr_2O_3	Corundum	Finger & Hazen (1980)
Karelianite	V_2O_3	Corundum	Finger & Hazen (1980)
Quartz	SiO_2	Quartz	d'Amour et al. (1979)
Quartz	SiO_2	Quartz	Levien et al. (1980)
Coesite	SiO_2	Coesite	Levien & Prewitt (1981 b)
Rutile	TiO_2	Rutile	Hazen & Finger (1980 a)
Cassiterite	SnO_2	Rutile	Hazen & Finger (1980 a)
—	RnO_2	Rutile	Hazen & Finger (1980 a)
—	GeO_2	Rutile	Hazen & Finger (1980 a)
—	MnF_2	Rutile	Hazen et al. (1978)
—	$Cs_2Au_2Cl_6$	Cesium Gold chloride	Denner et al. (1979)
Calcite	$CaCO_3$	Calcite	Merrill & Bassett (1975)
Pyrope	$Mg_3Al_2Si_3O_{12}$	Garnet	Hazen & Finger (1978 a)
Grossularite	$Ca_3Al_2Si_3O_{12}$	Garnet	Hazen & Finger (1978 a)
Forsterite	Mg_2SiO_4	Olivine	Hazen (1976 a)
Forsterite	Mg_2SiO_4	Olivine	Hazen & Finger (1980 b)
Fayalite	Fe_2SiO_4	Olivine	Hazen (1977 a)
—	Fe_2SiO_4	Spinel	Finger et al. (1979)
—	Ni_2SiO_4	Spinel	Finger et al. (1979)
Zircon	$ZrSiO_4$	Zircon	Hazen & Finger (1979 b)
Enstatite	$MgSiO_3$	Pyroxene	Ralph & Ghose (1980)
Diopside	$CaMgSi_2O_6$	Pyroxene	Levien & Prewitt (1981 a)
Fassaite	$(Ca,Mg,Fe,Ti,Al)_2(Si,Al)_2O_6$	Pyroxene	Hazen & Finger (1977 a)
Gillespite	$BaFeSi_4O_{10}$	Gillespite	Hazen & Burnham (1974, 1975)
Phlogopite	$KMg_3AlSi_3O_{10}F_2$	Mica	Hazen & Finger (1978 b)
Berndtite	SnS_2	Brucite	Hazen & Finger (1978 c)

* Early single-crystal studies at the National Bureau of Standards (Block et al., 1965; Weir et al., 1965, 1969 b, 1971; Piermarini & Braun, 1972) are not included because full structure refinements were not performed. Structure refinements of *powders* at high pressure by time-of-flight neutron diffraction (Jorgensen, 1978; Srinivasa et al., 1977, 1979; Cartz, 1979) are also omitted.

A consequence of eq. 8 is that a given type of polyhedron has nearly constant bulk modulus *independent* of structure. For example, magnesium-oxygen octahedra in MgO, orthosilicates, layer silicates, and chain silicates have the same bulk moduli (Fig. 9). Errors associated with polyhedral bulk moduli are often in excess of 10%, because bulk moduli are based on the differences between similar bond lengths. Even so, it appears that most polyhedra of a given

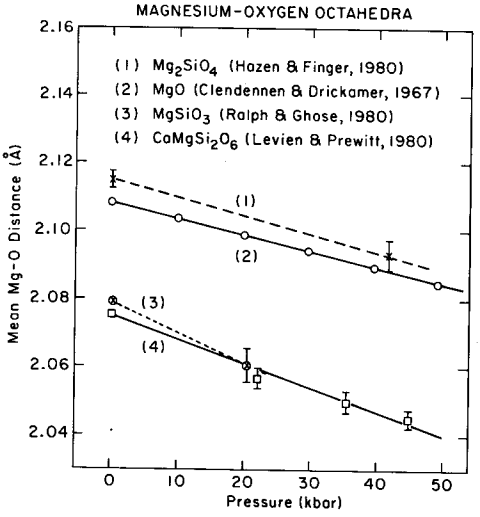

Fig. 9. Variation of Mg–O mean bond distance in magnesium-oxygen octahedra vs. pressure. In (4) the reference must read (Levien & Prewitt, 1981 a).

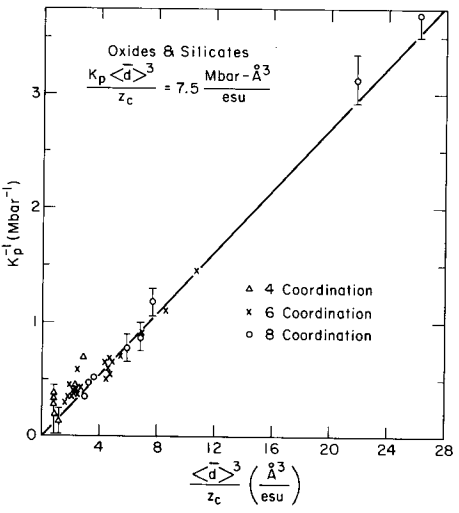

Fig. 10. The bulk modulus-volume relationship for cation-oxygen polyhedra in oxides and silicates (from Hazen & Finger, 1979 a).

type have bulk moduli within ± 15 % of each other. If polyhedral bulk moduli are independent of structure, then the high-pressure behavior of numerous materials, including glasses and other difficult-to-analyse structures, may be predicted.

The constancy of polyhedral bulk moduli in silicon tetrahedra may be questioned. High-pressure, single-crystal X-ray experiments have been limited to about 60 kbar, with a precision on Si–O distance no greater than 0.002 Å. It is not possible, therefore, to determine accurately the large (> 2.0 Mbar) bulk moduli of silicon tetrahedra. Although most authors agree that silicon tetrehedra are very rigid compared with monovalent or divalent cation polyhedra, it is not obvious whether all silicon tetrahedra have the same bulk modulus.

For oxides and silicates 38 polyhedral bulk moduli yield the relationship

$$K_{poly} \frac{\bar{d}^3}{z_c} = 7.5 \pm 0.2\,\text{Mbar}\,Å^3, \tag{9}$$

as illustrated in Fig. 10 (Hazen & Finger, 1979 a). A similar bulk modulus-volume relationship for halides is

$$K_{poly} \frac{\bar{d}^3}{z_c} = 5.6 \pm 0.1\,\text{Mbar}\,Å^3. \tag{10}$$

Eq. 9 for oxygen-based compounds and eq. 10 for halides may be combined with other data on sulfides, selenides, tellurides, phosphides, arsenides, antimonides, and carbides into a more general bulk modulus-volume relationship:

$$\frac{K_{poly}\bar{d}^3}{S^2 z_c z_a} = 7.5 \pm 0.2\,\text{Mbar}\,Å^3, \tag{11}$$

where z_a is the formal anion charge and S^2 is an empirical term for the relative "ionicity" of the

bond, defined as 0.50 for R^{2+}–O bonds in NaCl-type oxides. Eq. 11 implies that alkali cation polyhedra are more compressible than divalent cation octahedra, which are more compressible than tetrahedra of Al or Si. Eq. 11 is similar in form to eq. 5 of Anderson (1972, p. 278), which is valid for the *bulk* properties of several simple compounds. When applied to the bulk properties of minerals, however, a different constant may be required for each structure type. This difficulty is not present when eq. 11 is applied to cation coordination groups. A single constant appears to fit many different structure types, and the values of z_c and z_a are unambiguous.

Values of S^2 may be calculated from equations such as 9 and 10 for each type of anion. (Until a better measure of "ionicity" is available it will be assumed that S^2 is constant for a given anion.) If S^2 is defined to be 0.50 for all oxides and silicates, then combining eq. 10 and eq. 11 yields S^2 for halides ≈ 0.75. Empirical values of S^2 determined in this way for other anions are 0.40 for sulfides, selenides, and tellurides; 0.25 for phosphides, arsenides, and antimonides; and 0.20 for carbides.

Of the oxides and silicate polyhedra used to construct Fig. 10, those that deviate most from the empirical line are tetrahedra, such as Si in silicates and Zn in ZnO, and octahedrally coordinated vanadium in V_2O_3, an unusual oxide with metallic luster and conductivity. All these polyhedra, which are more compressible than indicated by eq. 9, also have bonding that is more covalent than that in the other plotted oxide and silicate polyhedra (i. e., S^2 may be less than 0.50). Thus, deviations from the line in Fig. 10 may provide an approximate measure of ionicity.

Fig. 11 illustrates eq. 11 for polyhedra in more than 100 substances in 19 different structure types. It is significant that a simple empirical relationship closely represents the bond compression in materials with a wide range of bond character and topology. Of the structure types examined, only CsCl is anomalous, with all four points falling significantly below the empirical line. The CsCl structure, with eight anions at the corners of a unit cube and a cation at the

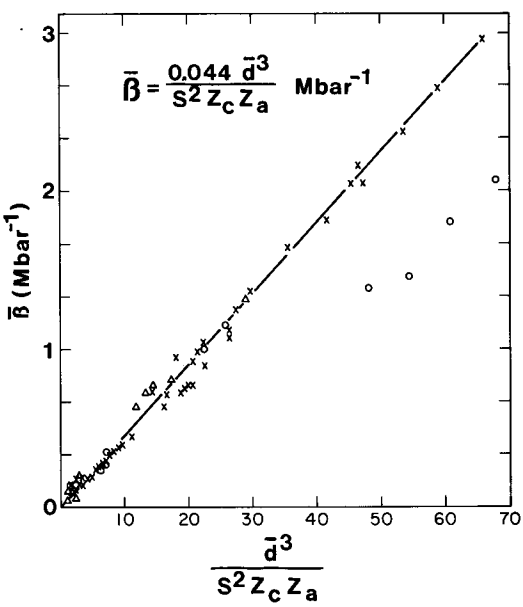

Fig. 11. The bulk modulus-volume relationship for cation polyhedra in a variety of compounds (from Hazen & Finger, 1979a).

cube's center, is unique in the high degree of face-sharing between adjacent polyhedra and the consequent short cation-cation separations. In CsCl-type compounds the cation-cation distance is only 15% longer than cation-anion bonds, in contrast to the 50–75% greater separation in most other structures. It is probable, therefore, that eq. 11, which incorporates only the bonding characteristics of the primary coordination sphere, is not valid for structures in which extensive face-sharing results in strong second-nearest neighbor interactions.

7. Polyhedral vs. bulk expansion and compression

Polyhedral thermal expansion and compressibility can be predicted from eqs. 5 and 11. In general, however, information on polyhedral size is not sufficient to predict bulk properties, because of the variety of polyhedral linkages. Distances and angles *between* polyhedra must also be considered.

Two cation polyhedra may be linked by a shared face, a shared edge, a shared corner, or Van der Wàal's forces. The type and distribution of these polyhedral linkages are the most important factors in determining the bulk thermal expansion or compression of a compound. The effects of different linkages on expansion or compression of two-dimensional analogs are illustrated in Fig. 12 (a–c). The degree to which mineral bulk volume changes differ from polyhedral volume changes depends on the rigidity of polyhedral linkages.

The most rigid polyhedral linkage is one in which polyhedra share faces or edges in three dimensions (Fig. 12a is a two-dimensional analog). If each shared edge between polyhedra is represented in space as a line segment, then all such line segments may form a continuous three-dimensional array. In these fully edge-linked structures (including rock salt, corundum, spinel, and garnet) any change in molar volume must be accompanied by a change in metal-oxygen distance because of rigid polyhedral linkages. Thermal expansion or compression of these compounds, consequently, is small because it is similar in magnitude to the thermal expansion or compression of metal-oxygen polyhedra. In rock salt- and corundum-type compounds, for example, the variations of the octahedra, the only polyhedra, and of the bulk compound are identical. In silicate spinels and garnets, having both silicate tetrahedra and

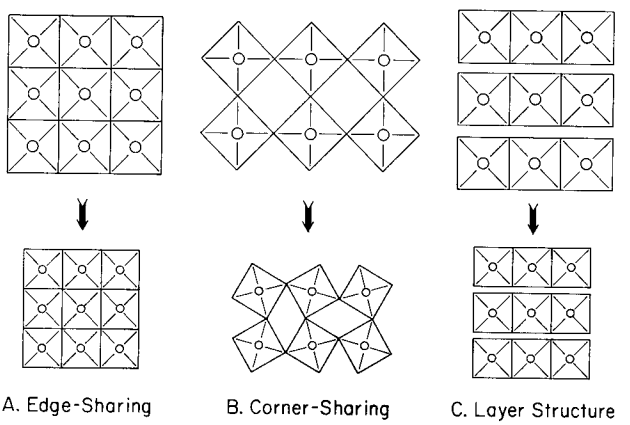

Fig. 12. Effects of polyhedral linkage on bulk compression or expansion. The square undergoes a constant area change in each of the three examples. Total area changes differ.

larger divalent cation polyhedra, the mineral expansivities and compressibilities are intermediate between the polyhedral variations of Si^{4+} and R^{2+} sites.

In contrast to fully edge-linked structures, some materials such as α-quartz, feldspar, and zeolites have primarily corner-linked polyhedra (Fig. 12b). In these framework structures volume changes may be effected by changes in angles between tetrahedra, without altering T–O distances. Framework silicates, consequently, have relatively large thermal expansion and compressibility, even though individual tetrahedra may undergo no volume change with temperature. The tilting of polyhedra in expansion or compression of corner-linked materials may be treated as primarily metal-oxygen-metal bond bending, as opposed to metal-oxygen bond expansion or compression.

In most structures, including layer silicates, chain silicates, and orthosilicates, polyhedra share edges with some adjacent polyhedra, link corners with others, and may have only weak Van der Waals attraction to still others (Fig. 12c). A continuous three-dimensional edge linkage does not obtain. In these materials expansion or compression is due to a combination of polyhedral (metal-oxygen) bond distance variations and bond bending, and the net expansion or compression is greater than that of component polyhedra. The significant differences in polyhedral linkages between the olivine and spinel forms of Mg_2SiO_4, for example, lead to the greater α and β of the former.

In summary, a knowledge of polyhedral expansion and compression does not lead directly to prediction of bulk mineral properties. Additional information, such as bond bending force constants, is needed. Nevertheless, qualitative predictions of bulk modulus and thermal expansion can be made.

8. Continuous variations of structure with temperature and pressure

8.1 The inverse relationship

Eq. 5, which relates thermal expansion to Pauling bond strength, implies that large alkali polyhedra expand more than divalent metal octahedra, which expand more than aluminum or silicon tetrahedra. Similarly, eq. 11 implies that large alkali sites compress more than divalent octahedra, which compress more than Al and Si tetrahedra. A direct consequence of eqs. 5 and 11, therefore, is that structural variations at high pressure often mirror those at high temperature. This "inverse relationship" has been observed in many minerals, including oxides, pyroxenes, feldspars, micas, olivines, and garnets. The inverse relationship is not always rigorously true. In diopside ($CaMgSi_2O_6$), for example, Ca and Mg have similar polyhedral expansion coefficients but different compressibilities. In other silicates, such as sanidine feldspar, however, the inverse relationship appears to hold extremely well, so that a structural change by heating may be exactly offset by compression.

8.2 The structural analogy of temperature, pressure, and composition

As noted above, an effect of temperature and pressure on structure is to alter the *ratio* of polyhedral sizes. The same type of structure variation may be achieved through cation substitution. In the alkali feldspar sanidine ($KAlSi_3O_8$), for example, an increase in pressure, a decrease in temperature, or a substitution of Na for K *all* have the same geometrical effect – the size of the alkali site is reduced relative to the Al and Si tetrahedra. In this geometrical sense, temperature, pressure, and composition may be structurally analogous variables (Hazen, 1977b).

In certain structures, such as sanidine, variations with temperature, pressure, and composition may all exactly offset each other. Aluminum and silicon tetrahedra show almost no size

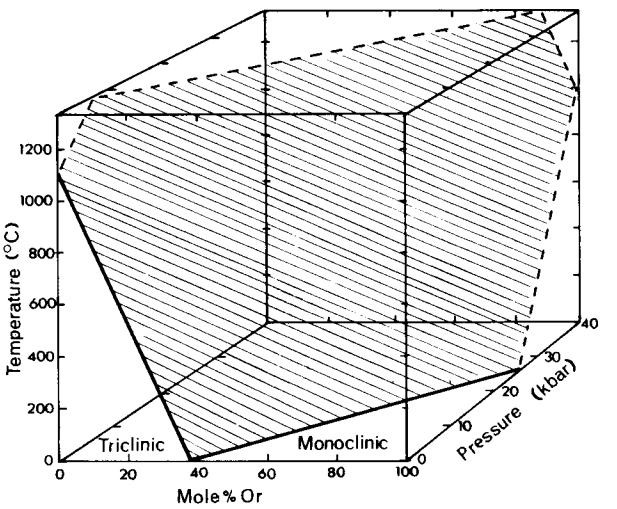

Fig. 13. Predicted phase transition surface for monoclinic-to-triclinic disordered alkali feldspars in the system $KAlSi_3O_8$ (Or)–$NaAlSi_3O_8$.

variations with T, P, or Na/K (at least in the range of crustal conditions). The size of the alkali site thus appears to define the feldspar structure in detail (Hazen, 1976c). The size of this large site is sensitive to changes in T, P, and Na/K. Consequently, there exist in T-P-X space surfaces of constant sanidine structure (i. e., constant cell constants and positional parameters), as illustrated in Fig. 13. Although few structures have isostructural surfaces in T-P-X space, all structures have T-P-X surfaces of constant *sub*structure (for example, constant polyhedral distortion). A knowledge of how polyhedral sizes vary with temperature, pressure, and composition may result in the prediction of these surfaces. Furthermore, in those instances where the stability of a phase is limited by the absolute or relative size of adjacent polyhedra it may be possible to predict phase equilibria.

9. Prediction of phase equilibria

One of the greatest challenges of solid-state science is the prediction of solid-solid phase equilibria. Although thousands of phase transitions have been documented experimentally, little success has been achieved in calculating the stability of crystalline matter from either theoretical or empirical models. It is possible, however, with concepts developed in the previous sections, to predict the stability of certain compounds that possess structures with geometrical limits. Phase transitions may occur in these compounds when adjacent structural elements (e. g., polyhedra) reach critical size limits by continuous variation with temperature, pressure, or composition.

Again the disordered alkali feldspar, sanidine, provides an excellent example (Hazen, 1976c). High sanidine ($KAlSi_3O_8$) is monoclinic, whereas high albite ($NaAlSi_3O_8$) is a distorted triclinic variant. For $K/(Na + K) < 0.40$, the alkali site is too small to support a monoclinic (Al, Si) framework, and a "collapsed" form results. A triclinic sanidine-type feldspar can be transformed to monoclinic by heating, by lowering pressure, or by increasing

K/(Na + K). The phase transition surface (Fig. 13) corresponds to a predictable surface of constant alkali site size, which in sanidine is also a surface of *constant* structure (Hazen, 1976c).

Several other examples of structures with geometrical limits are documented, including analcite (Hazen & Finger, 1979c), micas (Hazen & Wones, 1978), carbonates (Pauling, 1960), and chain silicates (Simons & Woermann, this volume). The prediction of phase equilibria from known structural limits remains an exciting field for further research.

10. Conclusions

Pauling's rules, formulated in the 1930's, were successful in modeling the geometry of numerous complex ionic materials with a relatively simple electrostatic concept of bonding. An implicit assumption of Pauling's rules is that the environment and properties of a cation are primarily a function of its nearest neighbors – the coordination polyhedra. The crystal chemistry of ionic solids at high temperature and pressure bears out this assumption to a remarkable degree. Polyhedral size, shape, thermal expansion, and compressibility are approximately independent of polyhedral linkages (i. e., second-nearest neighbors). Furthermore, the polyhedral compressibility and thermal expansivity may be calculated from the simplest of ionic bonding parameters: interionic distance, cation and anion formal charge, and coordination number. A major conclusion of crystallographic studies as a function of temperature, pressure, and composition is that the simple ionic model of bonding, as explored by Pauling, remains a valuable tool for the interpretation and analysis of structural geometry.

High-temperature, high-pressure crystallography is in its infancy. Three-dimensional structure refinements have been published for fewer than 50 materials at high temperature and fewer than 30 at high pressure. These results, though limited in scope, yield some remarkably simple and thought-provoking systematic relationships regarding the variation of structure with temperature, pressure, and composition.

References

Anderson, O. L. (1972): Patterns in Elastic Constants of Minerals Important to Geophysics. – In: Nature of the Solid Earth, 575–613, E. C. Robinson (ed.). New York, McGraw-Hill.

Anderson, O. L. & Anderson, O. L. (1970): The Bulk Modulus-Volume Relationship for Oxides. – J. Geophys. Res., **75,** 3494–3500.

Anderson, O. L. & Nafe, J. E. (1965): The Bulk Modulus-Volume Relationship for Oxide Compounds and Related Geophysical Problems. – J. Geophys. Res., **70,** 3951–3962.

Barnett, J. D., Block, S. & Piermarini, G. J. (1973): An Optical Fluorescence System for Quantitative Pressure Measurement in the Diamond Anvil Cell. – Rev. Sci. Instrum., **44,** 1–9.

Bassett, W. A. & Ming, L.-C. (1972): Disproportionation of Fe_2SiO_4 to $2FeO+SiO_2$ at Pressures up to 250 kbar and Temperatures up to 3000 °C. – Phys. Earth Planet. Interiors, **6,** 154–160.

Bassett, W. A. & Takahashi, T. (1965): Silver Iodide Polymorphs. – Amer. Miner., **50,** 1576–1594.

Block, S., Weir, C. E. & Piermarini, G. J. (1965): High Pressure Single Crystal Studies of Ice VI. – Science, **148,** 947–948.

Bridgman, P. W. (1923): The Compressibility of Thirty Metals as a Function of Temperature and Pressure. – Proc. Amer. Acad. Arts Sci., **58,** 165–242.

Brown, G. E. & Prewitt, C. T. (1973): High-Temperature Crystal Chemistry of Hortonolite. – Amer. Miner., **58,** 577–587.

Brown, G. E., Sueno, S. & Prewitt, C. T. (1973): A New Single-Crystal Heater for the Precession Camera and Four-Circle Diffractometer. – Amer. Miner., **58,** 698–704.

Cameron, M., Sueno, S., Prewitt, C. T. & Papike, J. J. (1973): High-Temperature Crystal Chemistry of Acmite, Diopside, Hedenbergite, Jadeite, Spodumene and Ureyite. – Amer. Miner., **58,** 594–618.

Cartz, L., Srinivasa, S. R., Riedner, R. J., Jorgensen, J. D. & Worlton, T. G. (1979): Effect of Pressure on Bonding in Black Phosphorous. – J. Chem. Phys., **71,** 1718–1721.

Clendenen, R. L. & Drickamer, H. G. (1966): Lattice Parameters of Nine Oxides and Sulfides as a Function of Pressure. – J. Chem. Phys., **44,** 4223–4228.

Cox, D. E. & Sleight, A. W. (1979): Mixed-Valent $Ba_2Bi^{3+}Bi^{5+}O_6$: Structure and Properties vs. Temperature. – Acta Crystallogr., **B35,** 1–10.

d'Amour, H., Denner, W. & Schulz, H. (1979): Structure Determination of α-Quartz up to 68×10^8 Pa. – Acta Crystallogr., **B35,** 550–555.

d'Amour, H., Schiferl, D., Denner, W., Schulz, H. & Holzapfel, W. B. (1978): High-Pressure Single-Crystal Structure Determinations of Ruby up to 90 kbar Using an Automatic Diffractometer. – J. Appl. Phys., **49,** 4411–4416.

Denner, W., Schulz, H. & d'Amour, H. (1979): The Influence of High Hydrostatic Pressure on the Crystal Structure of Cesium Gold Chloride ($Cs_2Au^IAu^{III}Cl_6$) in the Pressure Range up to 52×10^8 Pa. – Acta Crystallogr., **A35,** 360–365.

Finger, L. W. & Hazen, R. M. (1978): Crystal Structure and Compression of Ruby to 46 kbar. – J. Appl. Phys., **49,** 5823–5826.

–, – (1980): Crystal Structure and Isothermal Compression of Fe_2O_3, Cr_2O_3, and V_2O_3 to 50 kbar. – J. Appl. Phys., **51,** 5362–5367.

Finger, L. W., Hazen, R. M. & Yagi, T. (1979): Crystal Structures and Electron Densities of Nickel and Iron Silicate Spinels at Elevated Temperature or Pressure. – Amer. Miner., **64,** 1002–1009.

Finger, L. W. & King, H. (1978): A Revised Method of Operation of the Single-Crystal Diamond Cell and Refinement of the Structure of NaCl at 32 kbar. – Amer. Miner., **63,** 337–342.

Finger, L. W. & Ohashi, Y. (1976): The Thermal Expansion of Diopside to 800 °C and a Refinement of the Crystal Structure at 700 °C. – Amer. Miner., **61,** 303–310.

Foit, F. F. & Peacor, D. R. (1967): A High Temperature Furnace for a Single Crystal X-Ray Diffractometer. – Rev. Sci. Instrum., **44,** 183–185.

–, – (1973): The Anorthite Crystal Structure at 410° and 830°C. – Amer. Miner., **58,** 665–675.

Forman, N. & Peacor, D. R. (1970): Refinement of the Nepheline Structure at Several Temperatures. – Z. Kristallogr., **132,** 45–70.

Forman, R. A., Piermarini, G. J., Barnett, J. D. & Block, S. (1972): Pressure Measurement Made by the Utilization of Ruby Sharp-Line Luminescence. – Science, **176,** 284–285.

Fourme, R. (1968): Appareillage pour Etudes Radiocristallographiques sous Pression et à Température Variable. – J. Appl. Cryst., **1,** 23–30.

Glazer, A. M. & Mabud, S. A. (1978): Powder Profile Refinement of Lead Zirconate Titanate at Several Temperatures. II. Pure $PbTiO_3$. – Acta Crystallogr., **B34,** 1065–1070.

Goldschmidt, H. J. (1964): Bibliography 1: High-Temperature X-Ray Diffraction Techniques. – Utrecht, Internat. Union of Crystallography, Commission on Crystallographic Apparatus.

Hazen, R. M. (1976a): Effects of Temperature and Pressure on the Cell Dimension and X-Ray Temperature Factors of Periclase. – Amer. Miner., **61,** 266–271.

– (1976b): Effects of Temperature and Pressure on the Crystal Structure of Forsterite. – Amer. Miner., **61,** 1280–1293.

– (1976c): Sanidine: Predicted and Observed Monoclinic-to-Triclinic Reversible Transformations at High Pressure. – Science, **194,** 105–107.

– (1977a): Effects of Temperature and Pressure on the Crystal Structure of Ferromagnesian Olivine. – Amer. Miner., **62,** 286–295.

– (1977b): Temperature, Pressure, and Composition: Structurally Analogous Variables. – Phys. Chem. Minerals., **1,** 83–94.

Hazen, R. M. & Burnham, C. W. (1974): The Crystal Structures of Gillespite I and II: A Structure Determination at High Pressure. – Amer. Miner., **59,** 1166–1176.

–, – (1975): The Crystal Structure of Gillespite II at 26 kilobars: Correction and Addendum. – Amer. Miner., **60,** 937–938.

Hazen, R. M. & Finger, L. W. (1977a): Compressibility and Crystal Structure of Angra dos Reis Fassaite to 52 kbar. – Carnegie Inst. Washington Year Book, **76,** 512–515.

Hazen, R. M. & Finger, L. W. (1977b): Modifications in High-Pressure, Single-Crystal Diamond Cell Techniques. – Carnegie Inst. Washington Year Book, **76,** 655–656.
–, – (1978a): Crystal Structures and Compressibilities of Pyrope and Grossular to 60 kbar. – Amer. Miner., **63,** 297–303.
–, – (1978b): The Crystal Structures and Compressibilities of Layer Minerals at High Pressure. II. Phlogopite and Chlorite. – Amer. Miner., **63,** 293–296.
–, – (1978c): The Crystal Structure and Compressibilities of Layer Minerals at High Pressure. I. SnS_2, Berndtite. – Amer. Miner., **63,** 289–292.
–, – (1979a): Bulk Modulus-Volume Relationship for Cation-Anion Polyhedra. – J. Geophys. Res., **84,** 6723–6728.
–, – (1979b): Crystal Structure and Compressibility of Zircon at High Pressure. – Amer. Miner., **64,** 196–201.
–, – (1979c): Polyhedral Tilting: A Common Type of Phase Transition and Its Relationship to Analcite at High Pressure. – Phase Transitions, **1,** 1–22.
–, – (1980a): Bulk Moduli and High-Pressure Crystal Structures of Rutile-Type Compounds. – J. Phys. Chem. Solids, **42,** 143–151.
–, – (1980b): Crystal Structure of Forsterite at 40 kbar. – Carnegie Inst. Washington Year Book, **79,** 364–367.
–, – (1981): High-Temperature Diamond-Anvil Pressure Cell for Single-Crystal Studies. – Rev. Sci. Instrum., **52,** 75–79.
–, – (1982): Comparative Crystal Chemistry. – New York, Wiley International, in press.
Hazen, R. M., Finger, L. W. & Yagi, T. (1978): Crystal Structure and Compressibility of MnF_2 to 15 kbar. – Carnegie Inst. Washington Year Book, **77,** 841–842.
Hazen, R. M., Mao, H. K., Finger, L. W. & Bell, P. M. (1980): Crystal Structures and Compression of Ar, Ne, and CH_4 at 20 °C to 90 kbar. – Carnegie Inst. Washington Year Book, **79,** 348–351.
Hazen, R. M. & Prewitt, C. T. (1977): Effects of Temperature and Pressure on Interatomic Distances in Oxygen-Based Minerals. – Amer. Miner., **62,** 309–315.
Hazen, R. M. & Wones, D. R. (1978): Predicted and Observed Compositional Limits of Trioctahedral Micas. – Amer. Miner., **63,** 885–892.
Hochella, M. F., Brown, G. E., Ross, F. K. & Gibbs, G. V. (1979): High-Temperature Crystal Chemistry of Hydrous Mg- and Fe-Cordierites. – Amer. Miner., **64,** 337–351.
Horn, M., Schwerdtfeger, C. F. & Meagher, E. P. (1972): Refinement of the Structure of Anatase at Several Temperatures. – Z. Kristallogr., **136,** 273–281.
Jamieson, J. C., Lawson, A. W. & Nachtrieb, N. D. (1959): New Device for Obtaining X-Ray Diffraction Patterns from Substances Exposed to High Pressure. – Rev. Sci. Instrum., **30,** 1016–1019.
Jorgensen, J. D. (1978): Compression Mechanisms in α-Quartz Structures – SiO_2 and GeO_2. – J. Appl. Phys., **49,** 5473–5478.
Keller, R. & Holzapfel, W. B. (1977): Diamond Anvil Device for X-Ray Diffraction on Single Crystals under Pressures up to 100 kbar. – Rev. Sci. Instrum., **48,** 517–523.
Keller, R., Holzapfel, W. B. & Schulz, H. (1977): Effect of Pressure on the Atom Positions in Se and Te. – Phys. Rev., **B16,** 4404–4412.
King, H. E. (1978): Compression in Sulfide Crystal Structures: a Comparison with Oxides and Silicates. – Geol. Soc. Amer. Abstracts with Programs, **10,** 434.
King, H. E. & Finger, L. W. (1979): Diffracted Beam Crystal Centering and its Application to High-Pressure Crystallography. – J. Appl. Cryst., **12,** 374–378.
Lager, G. A. & Meagher, E. P. (1978): High-Temperature Structural Study of Six Olivines. – Amer. Miner., **63,** 365–377.
Levien, L. & Prewitt, C. T. (1981a): High-Pressure Structural Study of Diopside. – Amer. Miner., **66,** 315–323.
–, – (1981b): High-Pressure Crystal Structure and Compressibility of Coesite. – Amer. Miner., **66,** 324–333.
Levien, L., Prewitt, C. T. & Weidner, D. J. (1980): Single-Crystal X-Ray Study of Quartz at Pressure. – Amer. Miner., **65,** 920–930.
Mao, H. K. & Bell, P. M. (1976): High-Pressure Physics: The 1-Megabar Mark on the Ruby R_1 Pressure Scale. – Science, **191,** 851–852.

–, – (1980): Design and Operation of a Diamond-Window, High-Pressure Cell for the Study of Single-Crystal Samples Loaded Cryogenically. – Carnegie Inst. Washington Year Book, **79,** 409–411.

Meagher, E. P. (1975): The Crystal Structures of Pyrope and Grossularite at Elevated Temperatures. – Amer. Miner., **60,** 218–228.

Meagher, E. P. & Lager, G. A. (1979): Polyhedral Thermal Expansion in the TiO_2 Polymorphs: Refinement of the Crystal Structures of Rutile and Brookite at High Temperature. – Can. Miner., **17,** 77–85.

Megaw, H. D. (1938): The Thermal Expansion of Crystals in Relation to Their Structure. – Z. Kristallogr., **A100,** 58–76.

Merrill, L. & Bassett, W. A. (1974): Miniature Diamond Anvil Pressure Cell for Single Crystal X-Ray Diffraction Studies. – Rev. Sci. Instrum., **45,** 290–294.

–, – (1975): The Crystal Structure of $CaCO_3$. II. a High-Pressure Metastable Phase of Calcium Carbonate. – Acta Crystallogr., **B31,** 343–349.

Ming, L.-C. & Bassett, W. A. (1974): Laser Heating in the Diamond Anvil Press up to 2000 °C Sustained and 3000 °C Pulsed at Pressures up to 260 kbar. – Rev. Sci. Instrum., **45,** 1115–1118.

Moore, M. J., Sorensen, D. B. & DeVries, R. C. (1970): A Simple Heating Device for Diamond Anvil High Pressure Cells. – Rev. Sci. Instrum., **41,** 1665–1666.

Ohashi, Y. & Hadidiacos, C. G. (1976): A Controllable Thermocouple Microheater for High-Temperature Microscopy. – Carnegie Inst. Washington Year Book, **75,** 828–832.

Pauling, L. (1960): The Nature of the Chemical Bond. – Ithaca, New York, Cornell Univ. Press.

Peacor, D. R. (1973): High-Temperature Single-Crystal X-Ray Study of Natrolite. – Amer. Miner., **58,** 676–680.

Piermarini, G. J. & Braun, A. B. (1972): Crystal and Molecular Structure of CCl_4. III: A High Pressure Polymorph at 10 kbar. – J. Chem. Phys., **58,** 1974–1982.

Piermarini, G. J., Block, S. & Barnett, J. D. (1973): Hydrostatic Limits in Liquids and Solids to 100 kbar. – J. Appl. Phys., **44,** 5377–5382.

Piermarini, G. J., Block, S., Barnett, J. D. & Forman, R. A. (1975): Calibration of the Pressure Dependence of the R_1 Ruby Fluorescence Line to 195 kbar. – J. Appl. Phys., **46,** 2774–2780.

Pillars, W. W. & Peacor, D. R. (1973): The Crystal Structure of β-Eucryptite as a Function of Temperature. – Amer. Miner., **58,** 681–690.

Prewitt, C. T. (1976): Crystal Structures of Pyroxenes at High Temperature. – In: The Physics and Chemistry of Minerals and Rocks, R. G. J. Strens (ed.). New York, John Wiley.

Prewitt, C. T., Papike, J. J. & Ross, M. (1970): Cummingtonite: A Reversible, Nonquenchable Transition from $P2_1/m$ to C2/m Symmetry. – Earth Planet. Sci. Lett., **8,** 448–450.

Prewitt, C. T., Sueno, S. & Papike, J. J. (1976): The Crystal Structures of High Albite and Monalbite at High Temperatures. – Amer. Miner., **61,** 1213–1225.

Ralph, R. L. & Ghose, S. (1980): Enstatite, $Mg_2Si_2O_6$: Compressibility and Crystal Structure at 21 kbar. – Amer. Geophys. Union Trans. (EOS), **61,** V174.

Rice, C. E. & Robinson, W. R. (1977): High-Temperature Crystal Chemistry of Ti_2O_3: Structural Changes Accompanying the Semiconductor-Metal Transition. – Acta Crystallogr., **B33,** 1342–1348.

Robinson, W. R. (1975): High-Temperature Crystal Chemistry of V_2O_3 and 1% Chromium-Doped V_2O_3. – Acta Crystallogr., **B31,** 1153–1160.

Schiferl, D. (1977): 50-Kilobar Gasketed Diamond Anvil Cell for Single-Crystal X-Ray Diffractometer Use with the Crystal Structure of Sb up to 26 kilobars as a Test Problem. – Rev. Sci. Instrum., **48,** 24–30.

Smyth, J. R. (1969): Orthopyroxene-High-Low Clinopyroxene Inversions. – Earth Planet. Sci. Lett., **6,** 406–407.

– (1971): Protoenstatite: A Crystal-Structure Refinement at 1100 °C. – Z. Kristallogr., **134,** 262–274.

– (1972): A Simple Heating Stage for Single-Crystal Diffraction Studies up to 1000 °C. – Amer. Miner., **57,** 1305–1309.

– (1973): An Orthopyroxene Structure up to 850 °C. – Amer. Miner., **58,** 636–848.

– (1974): The High-Temperature Crystal Chemistry of Clinohypersthene. – Amer. Miner., **59,** 1069–1082.

– (1975): High Temperature Crystal Chemistry of Fayalite. – Amer. Miner., **60,** 1092–1097.

Smyth, J. R. & Burnham, C. W. (1972): The Crystal Structures of High and Low Clinohypersthene. – Earth Planet. Sci. Lett., **14,** 183–189.

Smyth, J. R. & Hazen, R. M. (1973): The Crystal Structures of Forsterite and Hortonolite at Several Temperatures up to 900 °C. – Amer. Miner., **58,** 588–593.

Srinivasa, S. R., Cartz, L., Jorgensen, J. D., Worlton, T. G., Beyerlein, R. A. & Billy M. (1977): High-Pressure Neutron Diffraction Study of Si_2Ni_2O. – J. Appl. Cryst., **10,** 167–171.

Srinivasa, S. R., Cartz, L., Jorgensen, J. D. & Labbe, J. C. (1979): Pressure-Induced Tetrahedral Tilting and Deformation in Ge_2Ni_2O. – J. Appl. Cryst., **12,** 511–516.

Sueno, S., Papike, J. J., Prewitt, C. T. & Brown, G. E. (1972): Crystal Structure of Cummingtonite. – J. Geophys. Res., **77,** 5767–5777.

Sueno, S., Cameron, M. E., Papike, J. J. & Prewitt, C. T. (1973): The High Temperature Crystal Chemistry of Tremolite. – Amer. Miner., **58,** 649–664.

Sueno, S., Cameron, M. E. & Prewitt, C. T. (1976): Orthoferrosilite: High Temperature Crystal Chemistry. – Amer. Miner., **61,** 38–53.

Sung, C.-M. (1976): New Modification of the Diamond Anvil Press: A Versatile Apparatus for Research at High Pressure and High Temperature. – Rev. Sci. Instrum., **47,** 1343–1346.

Takeda, H. & Morosin, B. (1975): Comparison of Observed and Predicted Structural Parameters of Mica at High Temperature. – Acta Crystallogr., **B31,** 2444–2452.

Taylor, M. & Brown, G. E. (1976): High-Temperature Structural Study of the $P2_1/a \rightleftarrows A2/a$ Phase Transition in Synthetic Titanite, $CaTiSiO_5$. – Amer. Miner., **61,** 435–447.

Van Valkenburg, A. (1963): High-Pressure Microscopy. – In: High-Pressure Measurements, 87–94, A. A. Giardini & E. C. Lloyd (eds.).

– (1964): Diamond High Pressure Windows. – Diamond Research, **1964,** 17–20.

Wechsler, B. A. (1977): Cation Distribution and High-Temperature Crystal Chemistry of Armalcolite. – Amer. Miner., **62,** 913–920.

Weir, C. E., Lippincott, E. R., Van Valkenburg, A. & Bunting, E. N. (1959): Infrared Studies in the 1- to 15-micron Region to 30,000 atmospheres. – J. Res. Nat'l. Bur. Standards (U. S.), **63A,** 55–62.

Weir, C. E., Block, S. & Piermarini, G. J. (1965): Single Crystal X-Ray Diffraction at High Pressure. – J. Res. Nat'l. Bur. Standards (U. S.), **69C,** 275–281.

Weir, C. E., Piermarini, G. J. & Block, S. (1969a): Instrumentation for Single Crystal X-Ray Diffraction at High Pressures. – Rev. Sci. Instrum., **40,** 1133–1136.

–, –, – (1969b): Crystallography of Some High-Pressure Forms of C_6H_6, CS_2, Br_2, CCl_4, and KNO_3. – J. Chem. Phys., **50,** 2089–2093.

–, –, – (1971): On the Crystal Structure of Cs-II and Ga-II. – J. Chem. Phys., **54,** 2768–2770.

Winter, J. K. & Ghose, S. (1979): Thermal Expansion and High-Temperature Crystal Chemistry of the Al_2SiO_5 Polymorphs. – Amer. Miner., **64,** 573–586.

Winter, J. K., Ghose, S. & Okamura, F. P. (1977): A High-Temperature Study of the Thermal Expansion and the Anisotropy of the Sodium Atom in Low Albite. – Amer. Miner., **62,** 921–931.

Winter, J. K., Okamura, F. P. & Ghose, S. (1979): A High-Temperature Structural Study of High Albite, Monalbite, and the Analbite-Monalbite Phase Transition. – Amer. Miner., **64,** 409–423.